AIP | Applied Physics Letters

# Spectral and angular distribution of Rayleigh scattering from plasmon-coupled nanohole chains

Yury Alaverdyan, Eva-Maria Hempe, A. Nick Vamivakas, Haibo E, Stefan A. Maier et al.

Citation: Appl. Phys. Lett. **94**, 021112 (2009); doi: 10.1063/1.3070520
View online: http://dx.doi.org/10.1063/1.3070520
View Table of Contents: http://apl.aip.org/resource/1/APPLAB/v94/i2
Published by the American Institute of Physics.

## Related Articles

Brillouin light scattering spectra as local temperature sensors for thermal magnons and acoustic phonons
Appl. Phys. Lett. 102, 082401 (2013)

Orientation correlation of p-nitroaniline molecules in acetone solution observed by hyper-Rayleigh scattering
J. Chem. Phys. 138, 054502 (2013)

Multi-modal characterization of nanogram amounts of a photosensitive polymer
Appl. Phys. Lett. 102, 024103 (2013)

Microscopic magnetic structuring of a spin-wave waveguide by ion implantation in a Ni81Fe19 layer
Appl. Phys. Lett. 102, 022409 (2013)

Hydrogen-terminated detonation nanodiamond: Impedance spectroscopy and thermal stability studies
J. Appl. Phys. 113, 023707 (2013)

## Additional information on Appl. Phys. Lett.

Journal Homepage: http://apl.aip.org/
Journal Information: http://apl.aip.org/about/about_the_journal
Top downloads: http://apl.aip.org/features/most_downloaded
Information for Authors: http://apl.aip.org/authors

ADVERTISEMENT

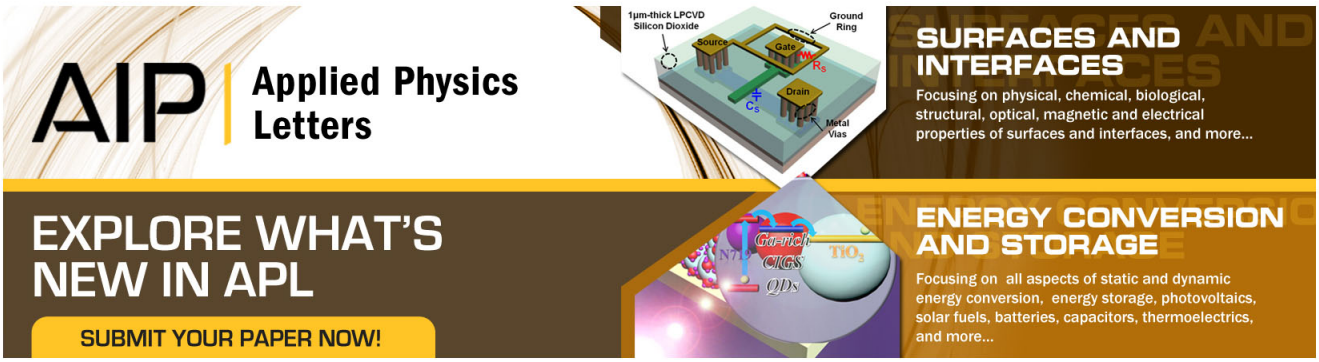

# Spectral and angular distribution of Rayleigh scattering from plasmon-coupled nanohole chains

Yury Alaverdyan,[1,a)] Eva-Maria Hempe,[1] A. Nick Vamivakas,[1] Haibo E,[1] Stefan A. Maier,[2] and Mete Atatüre[1,a)]
[1]*Cavendish Laboratory, University of Cambridge, Cambridge CB3 0HE, United Kingdom*
[2]*Physics Department, Blackett Laboratory, Imperial College London, Prince Consort Road, London SW7 2BZ, United Kingdom*

(Received 17 November 2008; accepted 20 December 2008; published online 14 January 2009)

We experimentally investigate the optical properties of nanohole chains in 20 nm gold films by measuring the far-field radiation patterns and scattering spectra using both white light and single-frequency laser excitations. We observe intensity enhancement in the frequency spectrum originating from resonantly coupled nanohole excitations via thin film surface plasmon polaritons. However, the angular distribution of the far-field pattern is identical to that of a chain of coherently radiating point dipoles both *on* and *off* the resonance frequency. We highlight a potential of the *k*-space imaging technique for studying far-field properties of ordered nanoscale structures. © *2009 American Institute of Physics*. [DOI: 10.1063/1.3070520]

The role of plasmons in the optical response of metallic nanostructures,[1] and, in particular, nanohole arrays have been under extensive study after the observation of extraordinary transmission (ET) of light through holes in *optically thick* metal films.[2] Surface plasmon polariton (SPP) modes of the metallic film,[3] or, in general, surface modes and their interplay with waveguide resonance in the nanoholes, as well as localized nanohole excitations,[4,5] have all been shown to take part in ET. In parallel, decreased divergence of the transmitted light has been observed for a number of ordered plasmonic structures via both near- and far-field manipulation. A single hole surrounded by Bull's eye structure[6,7] and a slit aperture with parallel grooves were reported to result in small divergence of the transmitted light,[8] and can be utilized to improve the directionality of quantum cascade lasers. Additionally, two-dimensional arrays of nanoholes were reported to enable focusing of light.[9]

While the above-mentioned results were obtained for thick metal slabs, it was recently shown that nanoholes arranged in short linear chains in *optically thin* metal films also display plasmonic effects.[10–13] Here, the optically active and propagating SPPs are in an antisymmetriclike modal profile ($a_b$-mode) formed between the air-metal and metal-dielectric boundaries, characterized by a symmetric charge distribution. It is suggested that this SPP mode can mediate a coupling mechanism between the neighboring holes via interference of the SPPs launched by each nanohole predominantly in the direction of polarization,[10,12] which was observed earlier for thicker films.[14] It was also suggested that SPPs may result in a narrowing of the far-field radiation pattern due to SPP cavities formed between the holes.[12] It is thus essential to have the ability to relate a far-field radiation pattern to the spectrum in order to resolve the underlying mechanism of the resonancelike intensity enhancement.

In this letter, we study the spectral and angular distributions of light scattered by a chain of ordered nanoholes as a function of interhole spacing and excitation wavelength. We show that the enhancement observed in spectral measurements arises from resonant interhole coupling via the thin film SPPs, while the angular distribution of the far-field pattern remains identical to that of a chain of coherently radiating point dipoles in the entire probed wavelength range. Our results demonstrate that the maximum coupling of light to surface plasmons and to outgoing scattered light by a nanohole chain occurs near the single hole resonance at the interhole distance ($d$) equal to half SPP wavelength. In contrast, the chains with the interhole distance other than half SPP wavelength show a strong deviation from the bare thin film SPP behavior away from the single hole resonance.

To determine the effect of plasmonic coupling on the beaming properties of nanohole chains, we constructed a microscope [see Fig. 1(a)] which images the back focal plane of the collecting objective in order to directly observe far-field radiation patterns. With the setup shown in Fig. 1(a) (top view), it is possible to measure a dark-field scattering spectrum, image the sample plane and image the back focal plane of the collection objective ($k$-space). In the excitation arm collimated white light from a 150 W halogen lamp or alternatively a 0.5 mW laser beam ($\lambda_{exc}$=532, 675, 780, or 968 nm) passes a near-infrared polarizer and a broadband half-wave plate before it is focused onto the sample by a condenser lens with a numerical aperture (NA) of 0.08. In spherical coordinates, the illumination of nanohole chains can be described as a weakly focused light beam at a polar angle $\theta$=65°, in order to maintain a dark-field regime, and an azimuthal angle $\varphi$=90° (perpendicular to a nanohole chain) so that all nanoholes in a chain are excited in phase [see Fig. 1(a) for details]. The light scattered by the sample is collected by a microscope objective (NA=0.7), split by a 50:50 beam splitter and sent to both, a fiber-optic single-grating spectrometer and two identical charge coupled device detectors which image the back focal plane ($k$-space) of the collecting objective and the sample surface.

Fabrication of the nanohole samples studied in this paper is published elsewhere.[13] The structures investigated here were circular nanoholes with a diameter of $D=100\pm5$ nm in $t$=20-nm-thick gold films where they were arranged in linear

a)Author to whom correspondence should be addressed. Electronic addresses: ya236@cam.ac.uk and ma424@cam.ac.uk.

 

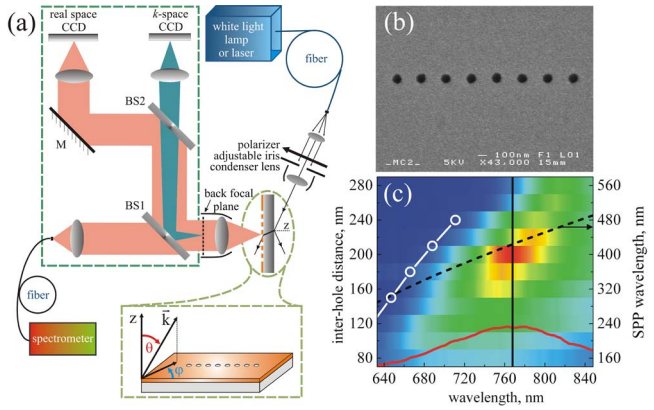


FIG. 1. (Color online) (a) Confocal optical microscope for simultaneously measuring spectra and imaging both sample surface and back focal plane of the collecting objective. (b) SEM image of a nanohole chain with $N=8$, $d=200$ nm. (c) A series of scattering spectra under white light illumination of $N=8$ nanohole chains for 11 different interhole distances within $d=80-280$ nm ($y$-axis on the left). The color red (blue) denotes high (low) intensity on the pseudocolor map, with maximum ~3600 counts. The dashed black curve represents the dependence of SPP wavelength on free-space wavelength ($y$-axis on the right) and the vertical black solid line at 765 nm marks the scattering peak position of a 100 nm single hole. The solid red curve is the corresponding single hole spectrum displaying the spectral width of the resonance. White open circles are the scattering peak positions for 60 nm nanohole chains for varied $d$, extracted from the results presented in Ref. 12.

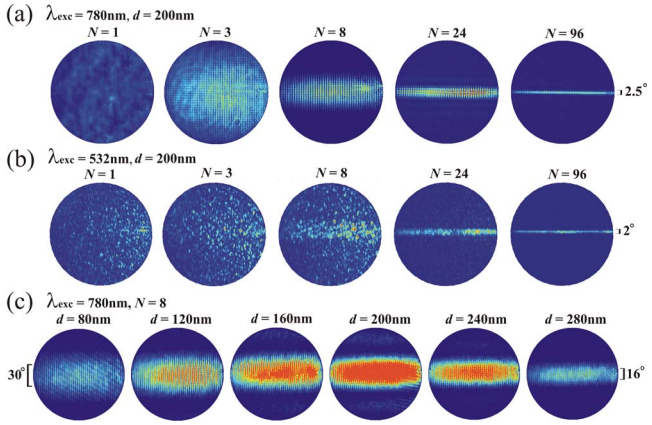


FIG. 2. (Color online) Measured far-field radiation patterns ($k$-space images) of the nanohole chains in pseudocolor map, where the color red (blue) denotes maximum (minimum) intensity. The full angular range is measured to be 89°. Narrowing of the pattern depending on the number of nanoholes per chain $N=1$, 3, 8, 24, and 96, $d=\lambda_{SPP}/2=200$ nm, with (a) $\lambda_{exc}=780$ nm, and (b) $\lambda_{exc}=532$ nm. (c) Series of $k$-space images taken with the same acquisition time at $\lambda_{exc}=780$ nm for a fixed number of holes $N=8$, for varying interhole distances $d=80-280$ nm. The fine fringes in the images originate from the propagation of highly coherent beams through imperfect optical elements, and are not related to beaming properties of the nanostructures.

chains. The edge-to-edge distance between two holes ($d$) was varied from 80 to 280 nm and the number of nanoholes per chain ($N$) was 1, 3, 8, 24, and 96. The samples were characterized by scanning electron microscopy (SEM) (JEOL JSM-6301F).

Figure 1(c) displays the scattering spectrum as a function of edge-to-edge interhole distance $d$ when the nanohole chains are excited by broadband white light polarized along the axis of the chains. Maximum scattering is found for $d \approx 200$ nm with a scattering peak position around 770 nm, close to the 100 nm single hole resonance peak position of 765 nm (indicated by the solid vertical black line). This free-space wavelength corresponds to $\lambda_{SPP} \approx 400$ nm of the $a_b$-mode, obtained from the dependence of the SPP wavelength on the free-space wavelength, calculated from the dispersion relation for the unperturbed thin film [dashed black line in Fig. 1(c)].[10,12,15] The white open circles are the scattering peak positions for $D=60$ nm chains $N=8$ (taken from Ref. 12) for varied interhole distance. The maximum scattering for the $D=60$ nm chains was found at 650 nm, close to the 60 nm single hole resonance peak position of 675 nm. Both observations are in good agreement with maximal scattering taking place for $d=\lambda_{SPP}/2$, exactly where SPPs interfere constructively. The redshift of the resonance with increasing interhole distance, as observed in earlier work, is also clearly visible. However, for wavelengths away from the single hole resonance, the condition for peak scattering intensity in nanohole chains does not coincide with the bare film SPP behavior [the dashed line in Fig. 1(c)], and peak position dependence on $d$ for $N=8$ chains of both 60 and 100 nm holes clearly deviates from the behaviour expected for the $a_b$-mode. This suggests that the presence of the coupled holes in the thin metal film modifies the bare SPP dispersion and that a more complete picture involving the hybridization of the nanohole resonances with the SPP modes is necessary to describe the nanohole chain scattering spectra.[11]

The deviation in Fig. 1(c) suggests that the interhole coupling may also have a signature in the far-field radiation pattern of the nanohole chain (directionality of radiation). To study the effect of SPP-mediated nanohole coupling on this pattern, we measured the angular distribution of the scattered light by using single-frequency laser excitation. Figures 2(a) and 2(b) display the far-field radiation pattern of the scattered light for a set of chains, arranged for the $d \approx 200$ nm $\approx \lambda_{SPP}/2$ condition, as a function of hole number ($N=1-96$). The general trend in beaming behavior holds for both *on*- and *off*-resonance excitation with $\lambda_{exc}=780$ nm [Fig. 2(a)] and 532 nm [Fig. 2(b)]. At the latter choice of excitation wavelength, sufficiently far away from the single hole resonance condition for launching thin film SPPs, no propagating modes between the holes are excited and the holes are expected to display no plasmon-induced coupling.[12,15] To model the observed beaming behavior, we compared the measured intensity angular distribution with the far-field radiation pattern of $N$ point dipoles, separated center to center by a distance $d+D$, driven with an excitation wavelength $\lambda_{exc}$ and radiating in phase. For comparison of the calculated radiation patterns with the measured intensity profiles we used the sine law to transform the dipole far field across the Gaussian reference sphere of the lens to a plane.[16] The slight difference between $\lambda_{exc}=780$ and 532 nm can be fully accounted for by the fact that the width of the central radiation lobe scales with $\lambda_{exc}/d$ in the point dipole model for a fixed $d \leqslant \lambda_{exc}$ and $N$. For the longest chain $N=96$ holes, the width of the central lobe narrows down to 2°. To emphasize the effect of plasmonic coupling on the scattering intensity, Fig. 2(c) shows the $k$-space images taken at $\lambda_{exc}=780$ nm as a function of interhole distance. The scattering intensity reaches a maximum at $d \approx \lambda_{SPP}/2$ (200 nm) coinciding with the resonance condition in Fig. 1(c). This is not the case for $\lambda_{exc}=532$ nm, for which the scattering intensity is substantially lower and exhibits no resonant behavior. In

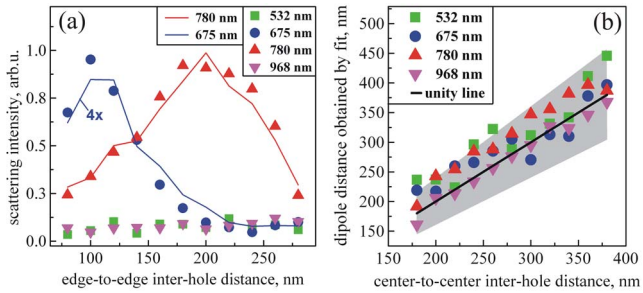


FIG. 3. (Color online) (a) Dependence of intensity of light scattered by the nanohole chains $N=8$ for different excitation wavelengths ($\lambda_{exc}=532$, 675, 780, and 968 nm) on the edge-to-edge distance between holes $d=80-280$ nm; the data points are extracted from $k$-space images; solid lines represent the data extracted from spectral measurements, shown in Fig. 1(c), for corresponding excitation wavelengths; the intensity data for $\lambda_{exc}=675$ nm is scaled by a factor of 4. (b) Comparison between beaming properties of nanohole chains and a modeled uniform chain of dipoles. Dipole-dipole distance obtained by fit to the model vs the actual center-to-center distance between the holes ($d+D$). The unity line is shown for comparison. Gray region shows the upper bound for the cumulative uncertainty resulting from fabrication, $k$-space measurements and data processing.

order to rule out diffractive effects in the angular distribution, we have also studied the complementary pattern of $N=8$ gold *nanodisks* as a function of disk separation. Neither the distance-dependent resonant behavior nor spectral shifts were also observed for these control samples.

Figure 3 investigates the dependence of scattering intensity and directionality on interhole distance for a number of excitation wavelengths, as extracted from the $k$-space images. In Fig. 3(a) the peak intensity values obtained from these $k$-space images (symbols) are in good agreement with those obtained from the direct spectral measurements (curves) [see Fig. 1(c)]. As can be seen, the chains exhibit a resonantlike behavior for the two laser wavelengths, $\lambda_{exc}=675$ and 780 nm, that are within the spectral envelope of the single hole resonance [Fig. 1(c)]. The 675 nm data are scaled by a factor of 4 to correct for this wavelength's detuning from the spectral location of peak scattering intensity. As expected from the dependence of the SPP wavelength on the excitation wavelength,[12] at $\lambda_{exc}=675$ nm the corresponding SPP wavelength is approximately 330 nm, much shorter than that at $\lambda_{exc}=780$ nm (430 nm). Surprisingly, the constructive interference ($d=\lambda_{SPP}/2$) occurs at $d=100$ nm rather than at 165 nm. This again is a direct consequence of the strong deviation from the thin film SPP behavior we observe in Fig. 1(c). Nevertheless, the qualitative agreement in Fig. 3(a) with the experimental data and the nanohole plasmon models reported earlier is apparent.[10,11]

To determine the effect of plasmonic coupling between the holes on the directionality of the scattered light, we fit the intensity profiles obtained from $k$-space images with the calculated far-field intensity profiles for a uniform chain of eight coherently radiating dipoles with the dipole-dipole distance being the fit parameter in Fig. 3(b). The unity-slope line highlights the expected behavior if the nanohole chains exhibit an angular distribution identical to a chain of point dipoles separated by $d+D$ (the gray area around this line indicates the upper bound of our experimental uncertainty). The dipole-dipole distance obtained from fitting to the model tells us how far apart the holes in a chain should be if they were point dipoles—if the structure displays a narrower radiation pattern then we would extract a $d$ which is *greater* than the actual interhole distance. In order to increase the signal-to-noise ratio in the experimental intensity distribution and to minimize the error introduced by a circular shape of the $k$-space images, the intensity profiles were based on the average of only 80 central vertical lines. Remarkably, we find that a chain of 100 nm nanoholes scatter light with the same directionality as a chain of *point* dipoles. Whereas we know that interaction of nanoholes via SPPs is present in the resonant behavior of the scattering intensity, it is clearly not accompanied by a modification of the radiation pattern.

To conclude, we studied the far-field scattering properties of hole chains in optically thin gold films with broadband and single-frequency excitation. We showed that despite the resonance-like scattering intensity modulation due to plasmonic coupling between holes, the radiation pattern of hole chanis remains identical to that of a chain of point dipoles, for both on and off resonance conditions. In addition, when detuned from the single hole resonance, the spectral response of hole chains strongly deviates from the thin film SPP dispersion.

The authors thank B. Sepúlveda for fruitful discussions. Fabrication was done at MC2 Nanofabrication Laboratory, Chalmers University of Technology, and was financed by the FP6-Research Infrastructures program MC2ACCESS through Contract No. 026029. The research leading to these results has received funding from the European Research Council (FP7/2007-2013)/ERC Grant agreement No. 209636, the internal funds of the University of Cambridge and EPSRC.

[1] S. A. Maier, *Plasmonics: Fundamentals and Applications* (Springer, New York, 2007).
[2] T. W. Ebbesen, H. J. Lezec, H. F. Ghaemi, T. Thio, and P. A. Wolff, Nature (London) **391**, 667 (1998).
[3] H. F. Ghaemi, T. Thio, D. E. Grupp, T. W. Ebbesen, and H. J. Lezec, Phys. Rev. B **58**, 6779 (1998).
[4] Z. C. Ruan and M. Qiu, Phys. Rev. Lett. **96**, 233901 (2006).
[5] K. L. van der Molen, K. J. Klein Koerkamp, S. Enoch, F. B. Segerink, N. F. van Hulst, and L. Kuipers, Phys. Rev. B **72**, 045421 (2005).
[6] H. J. Lezec, A. Degiron, E. Devaux, R. A. Linke, L. Martin-Moreno, F. J. Garcia-Vidal, and T. W. Ebbesen, Science **297**, 820 (2002).
[7] H. Caglayan, I. Bulu, and E. Ozbay, J. Opt. Soc. Am. B **23**, 419 (2006).
[8] N. Yu, J. Fan, Q. J. Wang, C. Pflügl, L. Diehl, T. Edamura, M. Yamanishi, H. Kan, and F. Capasso, Nat. Photonics **2**, 564 (2008).
[9] F. M. Huang, T. S. Kao, V. A. Fedotov, Y. F. Chen, and N. I. Zheludev, Nano Lett. **8**, 2469 (2008).
[10] T. Rindzevicius, Y. Alaverdyan, B. Sepúlveda, T. Pakizeh, J. Aizpurua, F. J. G. d. Abajo, and M. Käll, J. Phys. Chem. C **111**, 1207 (2007).
[11] T. H. Park, N. Mirin, J. B. Lassiter, C. L. Nehl, N. J. Halas, and P. Nordlander, ACS Nano **2**, 25 (2008).
[12] Y. Alaverdyan, B. Sepúlveda, L. Eurenius, E. Olsson, and M. Käll, Nat. Phys. **3**, 884 (2007).
[13] B. Sepulveda, Y. Alaverdyan, J. Alegret, M. Käll, and P. Johansson, Opt. Express **16**, 5609 (2008).
[14] E. S. Kwak, J. Henzie, S. H. Chang, S. K. Gray, G. C. Schatz, and T. W. Odom, Nano Lett. **5**, 1963 (2005).
[15] B. Sepulveda, L. A. Lechuga, and G. Armelles, J. Lightwave Technol. **24**, 945 (2006).
[16] L. Novotny and B. Hecht, *Principles of Nano-Optics* (Cambridge University Press, Cambridge, 2006).